

3D-QSAR study of hallucinogenic phenylalkylamines by using CoMFA approach

Zhuoyong Zhang · Liying An · Wenxiang Hu ·
Yuhong Xiang

Received: 4 July 2006 / Accepted: 22 October 2006 / Published online: 4 January 2007
© Springer Science+Business Media B.V. 2006

Abstract The three-dimensional quantitative structure–activity relationship (3D-QSAR) has been studied on 90 hallucinogenic phenylalkylamines by the comparative molecular field analysis (CoMFA). Two conformations were compared during the modeling. Conformation I referred to the amino group close to ring position 6 and conformation II related to the amino group trans to the phenyl ring. Satisfactory results were obtained by using both conformations. There were still differences between the two models. The model based on conformation I got better statistical results than the one about conformation II. And this may suggest that conformation I be preponderant when the hallucinogenic phenylalkylamines interact with the receptor. To further confirm the predictive capability of the CoMFA model, 18 compounds with conformation I were randomly selected as a test set and the remaining ones as training set. The best CoMFA model based on the training set had a cross-validation coefficient q^2 of 0.549 at five components and non cross-validation coefficient R^2 of 0.835, the standard error of estimation was 0.219. The model showed good predictive ability in the external test with a coefficient R^2_{pre} of 0.611. The CoMFA coefficient contour maps suggested that both steric and electrostatic interactions play an important role. The contributions from the steric and electrostatic fields were 0.450 and 0.550, respectively.

Keywords 3D-QSAR · Amphetamines · CoMFA · Hallucinogen · Phenylethylamines

Introduction

Hallucinogens are substances that provoke strong mental and psychic changes including disorientation, derealization and depersonalization, giving rise to a variety of abnormal phenomena [1]. In some countries, they are used as components of drugs. Some people especially young people show a special interest and may be addicted to these drugs for stimulation and self-realization effects. And more seriously, hallucinogens may be used to produce terror events by terrorists. To ensure the safety and the peace, strict administration and fast monitoring of hallucinogens are required.

Hallucinogens include mainly two categories of compounds according to their chemical structure. One is phenylalkylamines (phenylethylamines and amphetamines), and the other is indolealkylamines such as tryptamines and lysergic acid diethylamide (LSD) derivatives. The 5-HT_{2A} receptor is considered to act as the biological target of these compounds [2], however, the three-dimensional structure of 5-HT_{2A} receptor is not available so far, so most studies are based on homologous compounds. To understand the activity of hallucinogens at molecular level, their quantitative structure–activity relationships (QSARs) have been studied and several QSAR models have been established [3–7]. Most of the models were based on quantum chemistry parameters or physical chemistry parameters, and the computation based on quantum chemistry is slow and time-consuming.

Z. Zhang (✉) · L. An · W. Hu · Y. Xiang
Department of Chemistry, Capital Normal University,
105 Xisanhuan North, Beijing 100037, P.R. China
e-mail: gusto2008@vip.sina.com

Comparative Molecular Field Analysis (CoMFA) was developed by Cramer [8], and this method has been well established for ligand-based 3D-QSAR studies [9, 10]. It is based upon the calculated energies of steric and electrostatic interactions between the compound and the probe atom placed at the various intersections of a regular 3-D lattice. After this region is generated, the results are compared to the pharmacological data, and a linear combination of these two sets of data is constructed using a partial least squares (PLS) algorithm. Cross-validated and non-cross-validated r^2 -values are determined based on the PLS results in order to validate the predictive properties of the model. The r^2 -values can be optimized by iteratively varying the alignment rules, conformations and other parameters inherent to the technique.

In this paper, the 3D-QSAR models of 90 phenylalkylamines were established by CoMFA method. This general procedure has been used in the present study to gain insight into the steric and the electrostatic properties of these hallucinogenic phenylalkylamines, their influence on the activity and to derive predictive 3D-QSAR models for discovery and prediction of the hallucinogenic activities of new analogs for this class of hallucinogens.

Data set and methodology

Biological data

The structures of 90 phenylalkylamine compounds and the biological activities data were cited from the reference [5]. This biological data were collected by Shulgin and co-workers. The reported work was about the hallucinogenic effect on human (oral activity data) and it has been considered as a benchmark in QSAR studies. The activities (in Mescaline units) were the ratio of the effective dose of mescaline (350 mg) to the mean of the threshold dose of the trial drug and the dose required to obtain the full effect. In the following discussion, the alphabet *A* stands for the relative biological activity, Logarithm of *A* ($\log A$) was applied in the process of modeling. The structures and activity data of all the compounds were sorted by their structure character and were listed in Tables 1a, b and c, respectively. Eighteen compounds were randomly selected as test set marked with asterisks in the tables.

Molecular structure building and alignment

All computational studies were performed by the molecular modeling package sybyl 7.1 (Tripos Inc.,

USA) on a personal computer with Pentium IV processor. Molecular building was done with molecular sketch program. Since the crystal structure of DOET (4-ethyl-2,5-dimethoxyamphetamine) has been reported [11], the rest of the molecules were constructed using DOET as template. Active conformation selection is a key step for CoMFA analysis. Conformation with the lowest energy is not always the active conformation, and the proper active conformation can only be extracted from the crystal structure of the complex of the drug molecule and its binding receptor [12–13]. There are mainly two lower conformations for these compounds (Fig. 1), conformation I referred to the amino group close to ring position 6 and conformation II related to the amino group trans to the phenyl ring. Energy comparison showed that conformation I was more stable than conformation II. To better understand the activities of these compounds, the both conformations were used to build the models. The crystal conformation of DOET is similar to conformation I. The second conformation was acquired by interchange the positions of amino group and the methyl group (amphetamines) or hydrogen atom (phenylethylamines). Partial atomic charges were assigned to each atom and then energy minimization of each molecule was performed using Powell method and Tripos standard force field with a distance-dependent dielectric function. The minimization was terminated when the energy gradient convergence criterion of 0.005 kcal/mol was reached or when the 2000-step minimization cycle limit was exceeded.

Molecular alignment is considered as one of the most sensitive parameters in CoMFA analysis [14]. The quality and the predictive ability of the model are directly dependent on the alignment rule. Once the active conformation was determined, pharmacophore or common substructure alignment was carried out according to some rules. In this paper, common substructure alignment was carried out using database alignment tool with compound DOB as the template molecule (Fig. 2). To refine the superimposition, some molecules were manually adjusted using the rotation tools. Alignment of all compounds was shown in Fig. 3.

CoMFA analysis

In 3D-QSAR analysis, all aligned molecules were put into a 3D cubic lattice that extending at least 0.4 nm beyond the volumes of all investigated molecules on all axes. The region was partitioned into hundreds of grids with certain grid spacing. In the CoMFA analysis, Lennard-Jones 6–12 and Coulomb potentials were employed to calculate the CoMFA steric and

Table 1 Structure and hallucinogenic activity of (a) Phenylethylamines, (b) amphetamines and (c) some specially substituted compounds

No	Designation	R	A	Log A
<i>(a) Phenylethylamines [5]</i>				
1	Mescaline	3,4,5-trimethoxy	1	0.00
2	ME*	3-ethoxy-4, 5-dimethoxy	1	0.00
3	E	3,5-dimethoxy-4-ethoxy	6	0.78
4	P	3,5-dimethoxy-4-propoxy	7	0.85
5	ASB	3,4-diethoxy-5-methoxy	1.3	0.11
6	2C-E	2,5-dimethoxy-4-ethyl	18	1.26
7	2C-D	2,5-dimethoxy-4-methyl	8	0.90
8	3-TM	3,4-dimethoxy-5-methylthio	4	0.60
9	TM	3,5-dimethoxy-4-methylthio	10	1.00
10	3-TME	3,4-dimethoxy-5-ethylthio	4	0.60
11	4-TME	3-ethoxy-4-methylthio-5-methoxy	4	0.60
12	3-TE*	3-methoxy-4-ethoxy-5-methylthio	4	0.60
13	4-TE	3,5-dimethoxy-4-ethylthio	12	1.08
14	3-TASB	3-ethylthio-4-ethoxy-5-methoxy	2	0.30
15	4-TASB	3-ethoxy-4-ethylthio-5-methoxy	4	0.60
16	5-TASB*	3,4-diethoxy-5-methylthio	2	0.30
17	TP	3,5-dimethoxy-4-propylthio	16	1.20
18	TB	3,5-dimethoxy-4-butylthio	3	0.48
19	2C-G	2,5-dimethoxy-3,4-dimethyl	11	1.04
20	2C-T-F*	2,5-dimethoxy-4-(2-fluoroethylthio)	29	1.46
21	2C-T-13	2,5-dimethoxy-4-(2-methoxyethylthio)	9	0.95
22	2C-B*	2,5-dimethoxy-4-bromo	16	1.20
23	2C-I	2,5-dimethoxy-4-iodine	17	1.23
24	2C-C	2,5-dimethoxy-4-chloro	10	1.00
25	CPM	3,5-dimethoxy-4-cyclopropylmethoxy	4	0.60
26	IP	3,5-dimethoxy-4-(i)-propoxy	5	0.70
27	BOD*	4-methyl-2,5, β -trimethoxy	15	1.18
28	BOH	β -methoxy-3,4-methylenedioxy	3	0.48
29	2C-P	2,5-dimethoxy-4- <i>n</i> -propyl	37	1.57
30	2C-T*	2,5-dimethoxy-4-methylthio	4	0.60
31	2C-T-2	2,5-dimethoxy-4-ethylthio	16	1.20
32	2C-T-4	2,5-dimethoxy-4-isopropylthio	21	1.32
33	2C-T-7	2,5-dimethoxy-4- <i>n</i> -propylthio	15	1.18
34	2C-T-8	2,5-dimethoxy-4-cyclopropylmethylthio	7	0.85
35	2C-T-9	2,5-dimethoxy-4-tert-butylthio	4	0.60
36	2C-T-17	2,5-dimethoxy-4-sec-butylthio	4	0.60
37	HOT-2*	2,5-dimethoxy-4-ethylthio- <i>N</i> -hydroxy	22	1.34
38	HOT-7	2,5-dimethoxy- <i>N</i> -hydroxy-4- <i>n</i> -propylthio	15	1.18
39	HOT-17	2,5-dimethoxy-4-sec-butylthio- <i>N</i> -hydroxy	3	0.48
40	BOB	2,5, β -trimethoxy-4-bromo	20	1.30
41	DESOXY	3,5-dimethoxy-4-methyl	4	0.60
42	MAL	3,5-dimethoxy-4-methylthio	6	0.78
43	MDPH	α , α -dimethyl-3, 4-methylenedioxy	1.5	0.18
<i>(b) Amphetamines</i>				
44	4-MA*	4-methoxy	5	0.70
45	2,5-DMA	2,5-dimethoxy	2.5	0.40
46	TMA	3,4,5-trimethoxy	2	0.30
47	TMA-2	2,4,5-trimethoxy	10	1.00
48	TMA-4	2,3,5-trimethoxy	4	0.60
49	TMA-5	2,3,6-trimethoxy	10	1.00
50	TMA-6*	2,4,6-trimethoxy	10	1.00
51	MEM*	2,5-dimethoxy-4-ethoxy	9	0.95
52	3C-BZ	3,5-dimethoxy-4-benzoyloxy	3	0.48
53	TA	2,3,4,5-tetramethoxy	6	0.78
54	MDA*	3,4-methylenedioxy	3	0.48
55	MMDA	3-methoxy-4, 5-methylenedioxy	2	0.30
56	MMDA-2	2-methoxy-4, 5-methylenedioxy	8	0.90
57	MMDA-3A	2-methoxy-3, 4-methylenedioxy	6	0.78
58	DMMDA	2,5-dimethoxy-3, 4-methylenedioxy	6	0.78
59	DOM	2,5-dimethoxy-4-methyl	50	1.70

Table 1 continued

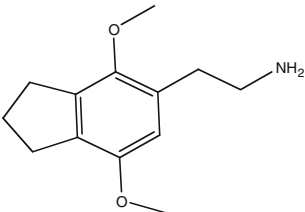
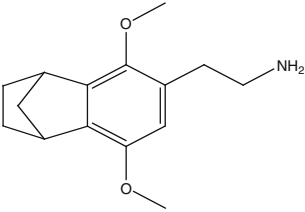
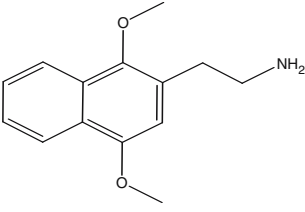
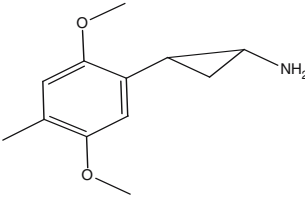
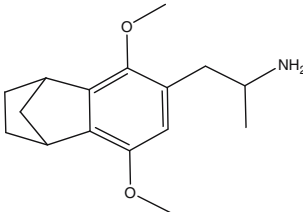
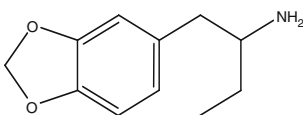
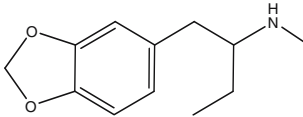
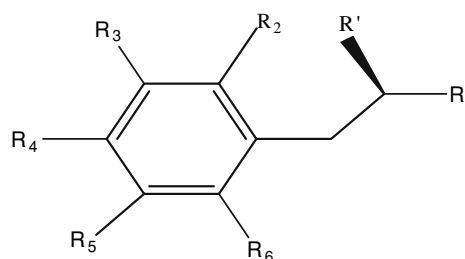
No	Designation	R	A	Log A
60	DOET	2,5-dimethoxy-4-ethyl	75	1.88
61	DOEF	2,5-dimethoxy-4-(2-fluoroethyl)	110	2.04
62	DOPR*	2,5-dimethoxy-4- (n)-propyl	80	1.90
63	PARADOT	2,5-dimethoxy-4-methylthio	40	1.60
64	ALEPH-4	2,5-dimethoxy-4-(i)-propylthio	32	1.51
65	DOB	2,5-dimethoxy-4-bromo	150	2.18
66	DOI*	2,5-dimethoxy-4-iodine	133	2.12
67	DOC	2,5-dimethoxy-4-chloro	133	2.12
68	DON	2,5-dimethoxy-4-nitro	80	1.90
69	AL	3,5-dimethoxy-4-allyloxy	11	1.04
70	ALEPH-2*	2,5-dimethoxy-4-ethylthio	50	1.70
71	Ψ-DOM	2,6-dimethoxy-4-methyl	15	1.18
72	4-Br-3,5-DMA*	3,5-dimethoxy-4-bromo	43	1.63
73	FLEA	N-hydroxy-N-methyl-3,4-dimethylenedioxy	2.5	0.40
74	G-3	2,5-dimethoxy-3,4-trimethylene	20	1.30
75	G*	2,5-dimethoxy-3,4-dimethyl	12	1.08
76	MDE	3,4-methylenedioxy-N-ethyl	2	0.30
77	MDOH	3,4-methylenedioxy-N-hydroxy	2.3	0.36
78	5-TOET	4-ethyl-2-methoxy-5-methylthio	15	1.18
79	2-TOM	5-methoxy-4-methyl-2-methylthio	4	0.60
80	5-TOM	2-methoxy-4-methyl-5-methylthio	7	0.85
81	ALEPH-7	4-propylthio-2,5-dimethoxy	55	1.74
82	3C-E	3,5-dimethoxy-4-ethoxy	7	0.85
83	META-DOB	2,4-dimethoxy-5-bromo	4	0.60
(c) Some specially substituted compounds				
84	2C-G-3		14	1.15
85	2C-G-5		22	1.34
86	2C-G-N		10	1.00
87	DMCPA		17	1.23

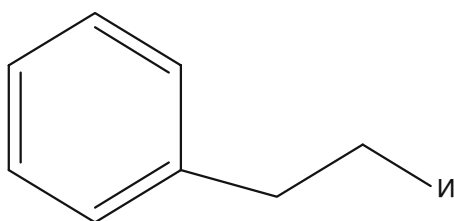
Table 1 continued

No	Designation	R	A	Log A
88	G-5		18	1.26
89	J*		1.5	0.18
90	Methyl-J		1.5	0.18



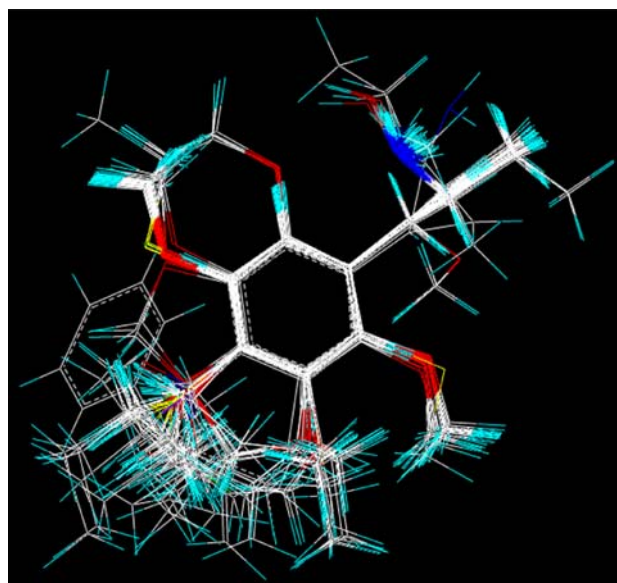
Conformation I: R' = NH₂, R = CH₃/H

Conformation II: R' = CH₃/H, R = NH₂

Fig. 1 Structure of phenylalkylamines**Fig. 2** Basic substructure for alignment

electrostatic interaction fields, respectively. An sp³-hybridized carbon atom with a charge of +1 was used as the probe atom and the steric and electrostatic energy cutoff was 30 kcal/mol and column-filtering value set to 1.0 cal/mol.

Partial least squares method was carried out with the leave-one-out (LOO) cross-validation procedure to determine the optimum number of components for the final non-cross-validated 3D-QSAR models. The opti-

**Fig. 3** Alignment of compounds in the training set

mal number of components produces the smallest root mean predictive sum of squared errors, which usually corresponds to the highest cross-validated squared coefficient (q^2) $q^2 = 1 - \frac{\sum (Y_{\text{obs}} - Y_{\text{pre}})^2}{\sum (Y_{\text{obs}} - Y_{\text{mean}})^2}$. The predictive power of the resulting 3D-QSAR models was assessed on the holdout test set using the R_{pre}^2 metric defined as $R_{\text{pre}}^2 = \frac{\text{SD} - \text{PRESS}}{\text{SD}}$, where SD is defined as the sum of squared deviations between the biological activities of the test set and the mean value of the training set responses, and PRESS is the sum of the squared deviation between the predicted and experimental bioactivities for the test compounds.

Results and discussion

Conformation analysis

The statistical results of the two models from different conformations were summarized in Table 2. It suggested that both CoMFA models have predictive ability ($q^2 > 0.50$). Contributions of the steric and electrostatic fields in the two models were almost the same. But the model based on conformation I was a little better. This may suggest that conformation I should be preponderant when the ligands interacted with the 5-HT_{2A} receptor. And this hypothesis was in agreement with Nichols' work.

Nichols et al. have developed a homology model of the 5-HT_{2A} receptor based on an in silico activated form of bovine rhodopsin [15]. When mescaline was docked into this model, it was observed that the 3- and 5-methoxy groups adopted out-of-plane conformations allowing hydrogen bonding with serine residues, and the side chain was in an approximately gauche conformation. Next, they synthesized a more conformationally restricted compound, which maintains the embedded mescaline structure in a low-energy conformation and docked this molecule to the 5-HT_{2A} homology. And it also showed that the amine-bearing side chain adopts a gauche orientation upon binding to the receptor [16]. So, we can conclude that conformation I is more favorable.

Selection of grid spacing

The influence of different grid spacing was investigated and the results were listed in Table 2. It can be concluded from Table 3 that grid spacing affected the model to certain extent. If grid spacing is too large, the grids become sparse, which may cause some important molecular field information being unable to be well

Table 2 The statistic results of the two conformations

Statistic index	Conformation I	Conformation II
N	7	7
q^2	0.640	0.596
R^2	0.879	0.849
s	0.187	0.209
F	85.102	65.914
Contributions %		
Steric	45.0	45.2
Electrostatic	55.0	54.8

Note: q^2 is the cross-validated squared coefficient, N is the optimal number of components, R^2 is the non cross-validated squared coefficient, s is the standard error of estimation and F is the F -test value

Table 3 The influence of different grid spacing

Grid spacing	q^2	N	R^2	s	F
1.0	0.669	6	0.858	0.201	83.789
1.5	0.649	6	0.847	0.209	76.453
2	0.640	7	0.879	0.187	85.102
2.5	0.589	6	0.810	0.232	59.147

Notations are the same as Table 2

expressed. In this paper, smaller step size increased the q^2 value but not very significantly. Moreover, smaller step size dramatically increased the computation and much more time was involved. So grid spacing was set to 0.2 nm in the following modeling.

Selection of charge calculation method

In this paper, four charge calculation methods including Gasteiger–Marsili, Pullman, Gasteiger–Hückle and MMFF94 were compared. The results in Table 4 showed that Gasteiger–Hückle and MMFF94 charge got better results than the other two. The worst results were obtained with Gasteiger–Marsili charge method. This case may be due to the Gasteiger–Marsili charge only accounts for σ electron, but both σ and π electrons contribute to the interactions between receptor and ligand molecules. MMFF94 charge brought a larger standard error than Gasteiger–Hückle charge, so Gasteiger–Hückle charge was utilized.

CoMFA results

The statistical results of the two models were summarized in Table 2. It suggested that both CoMFA models had predictive ability ($q^2 > 0.50$). But the model from conformation I got higher q^2 value than the other one by nearly 10%. Both of the models got good results at seven principal components. And there is little difference between the non cross-validation coefficients. But the model I got a much smaller standard error of estimation. Contributions of the steric and electrostatic fields in the two models were almost the same. But the model based on conformation I was a little better. To further study the predictive ability of this model, 18

Table 4 The influence of different charge calculation methods

Charge	q^2	N	R^2	s	F
Gasteiger–Hückle	0.640	7	0.879	0.187	83.789
Gasteiger–Marsili	0.445	7	0.875	0.184	63.985
Pullman	0.489	6	0.815	0.222	47.843
MMFF94	0.605	6	0.840	0.209	59.175

Notations are the same as Table 2

compounds were randomly selected as the test set and the remaining as the training set. The best model had a q^2 of 0.549 at five components, non cross-validation squared coefficient of 0.835 and standard error of estimated value of 0.219. For the prediction of the holdout test compounds the R^2_{pre} was 0.611, these statistical results confirmed the predictive capacity of the resultant CoMFA model. The predictive values of the holdout test compounds were listed in Table 5. The best CoMFA model was represented in Fig. 4, which shows the correlation of experimental values versus the predicted values for compounds both in the training

Table 5 Actual value and the corresponding predicted values for the test compounds (activities are in Mescaline unit)

Compounds	Actual	Predicted	Residue
2C-B	1.204	1.199	0.005
2C-T	0.602	1.062	-0.460
2C-T-F	1.462	1.748	-0.286
3-TE	0.602	0.482	0.120
4-Br-3, 5-DMA	1.634	1.073	0.561
4-MA	0.699	0.667	0.032
5-TASB	0.301	0.235	0.066
ALEPH-2	1.699	1.622	0.077
BOD	1.176	1.064	0.112
DOI	2.124	1.846	0.278
DOPR	1.903	1.819	0.084
G	1.08	1.024	0.056
HOT-2	1.34	1.028	0.312
J	0.179	0.254	-0.075
MDA	0.477	0.255	0.222
ME	0	0.237	-0.237
MEM	0.954	1.303	-0.349
TMA-6	1	1.627	-0.627

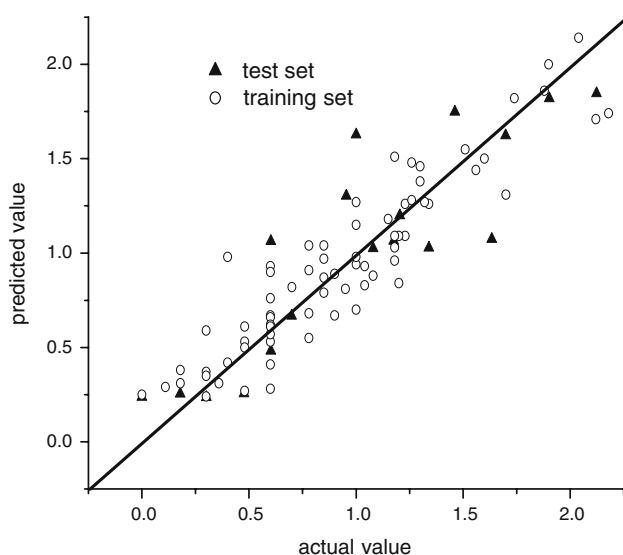


Fig. 4 Predicted versus actual value of compounds both in training and test set for the best CoMFA model

and test sets. In Fig. 4, most points evenly distributed among the line $Y = X$, which suggested the good quality of the models.

CoMFA coefficient contour map analysis

Figure 5 showed the steric and electrostatic fields of compound ME ($A = 1$ MU, Mescaline Unit) and DOEF ($A = 110$ MU) based on the CoMFA model of the 90 compounds. The green contours characterize the regions where bulky substituents would increase the biological activity, whereas yellow contours indicate regions where steric bulk would not be tolerated. The blue and red polyhedra depict the favorable sites for positively and negatively charged groups, respectively. The green polyhedron located at the 4-position of the phenyl ring indicates that bulky substituents would be favorable. This can explain compound E (only ethoxy substitutes of methoxy in molecule Mescaline at the 4-position) is five times higher than Mescaline. At the 3-position, there is a relatively large yellow region, so

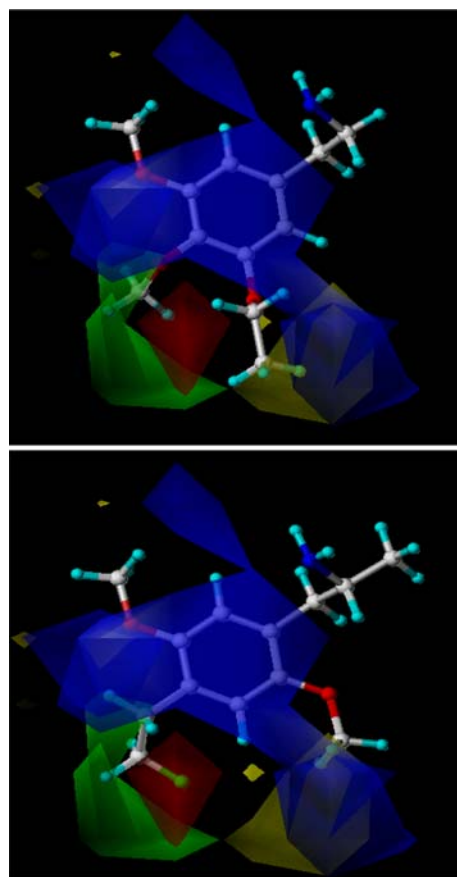


Fig. 5 Contour maps of the steric and electrostatic field of molecule ME (with low activity) and DOEF (with high activity) based on the whole CoMFA model

ME with an ethoxy group at 3-position has activity the same as Mescaline. The large blue polyhedra encircling the benzene ring at the meta-positions indicate negatively charged elements for meta-substitution on phenyl ring were unfavorable, which appears to account for the poor activity of some compounds with methylenedioxy-substituents such as MDE, MDOH, J, and BOH, etc. The red polyhedron located at the 4-position of the phenyl ring suggests that negative atom or group may increase activity, so, the electron-rich groups and atoms at this position (such as DOEF, DOB, DOC, and DON) show strong hallucinogenic activity. Figure 5 distinctly showed the F atom located in the red polyhedron. However, predictive values for 4-halide substituted compounds such as DOB and DOC were a little lower than the actual values. These results showed that there might exist other factors influencing the overall activities. And there is evidence that substituent at the 4-position of various phenylisopropylamines might directly interact with receptors [17]; Hydrophobicity effect of the 4-position is crucial to the hallucinogenic activity. Domelsmith et al. have examined a series of 13 phenylisopropylamine derivatives, which revealed a correlation ($r^2 = 0.81$) between their hallucinogenic potencies and the lipophilic values of their 4-position substituents [18].

There is another noticeable phenomenon that the molecule TM with methylthio substituent at the 4-position of the phenyl ring has much higher activity than Mescaline ($A = 10$ MU). So it can be proposed that alkylthio-substituent at the 4-position is favorable for the hallucinogenic activity. This “thio-effect” may result from the change of the orbital hybridization of the heteroatom and therefore a change of the availability of the molecule to metabolism [19].

From the contour map, it can be found that substituents at the para- and meta- positions were crucial to the hallucinogenic activity of these compounds. So modifications can be focused on these positions. And also we can presume that there may be other factors that affect the hallucinogenic activity.

To validate the established model, two separately synthesized potential hallucinogenic compounds [20] (Figure 6) were used for prediction. The predicted values suggest that compound 2 have higher activity than compound 1. This result is consistent with the conclusion from reference [20]. It was reported in the reference [20] that compound 2 has an approximately 60-fold higher affinity than the compound 1 in vitro assays. In the rat drug discrimination assay, the compound 2 is three times more potent than the compound 1. The predicted hallucinogenic activity data of the two compounds from our model is 0.446 and 1.347,

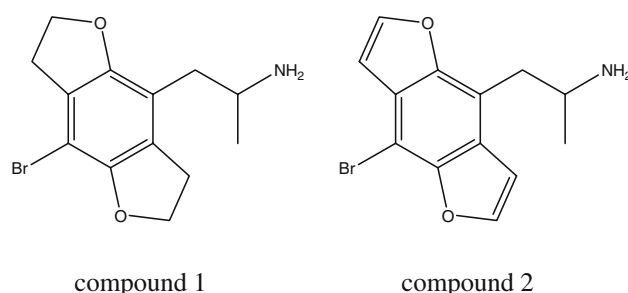


Fig. 6 Structures of two newly synthesized potential hallucinogens

respectively. This similarity further conformed the predictive ability of the model.

Conclusions

In this study, CoMFA model has been created to explain the observed structure–activity relationship for a series of hallucinogenic phenylalkylamines. Two conformations were compared and the best model was achieved by the lower conformation (conformation I). Several parameters were discussed in the optimization of the model. The results of the holdout test showed that this model had predictive ability. The coefficient contour map showed that both steric and electrostatic fields play an important role, their contributions were 45.0% and 55.0%, respectively. Rational explanations of the structure–activity relationship of these compounds were reached from the contour map. This offered important information for further structure modification and discovery new potential hallucinogenic phenylalkylamines.

Acknowledgements This work is supported by the Science and Technology Program of Beijing Municipal Government and the Scientific Research Common Program of Commission of Education.

References

- Nichols DE (2004) *Pharmacol Ther* 101:131
- Krebs-Thomson K, Paulus MP, Geyer MA (1998) *Neuropsychopharmacology* 18:339
- Nichols DE (1981) *J Pharm Sci* 70:839
- Gupta SP, Singh P, Bindal MC (1983) *Chem Rev* 83:633
- Clare BW (1990) *J Med Chem* 33:687
- Clare BW (2002) *Computer-Aided Mol Des* 16:611
- Schulze-Alexandru M, Kovar K-A (1999) *Quant Struct-Act Relat* 18:548
- Cramer RD, Patterson DE, Bunce JD (1988) *J Am Chem Soc* 110:5959
- Klebe G, Abraham U, Mietzner T (1994) *J Med Chem* 37:4130
- Song MH, Breneman CM, Sukumar N (2004) *Bioorg Med Chem* 12:489

11. Kennard O, Giacobozzo C, Horn AS, Mongiorgi R, Riva di Sanseverino L (1974) *J Chem Soc Perkin Trans II* 10:1160
12. Hu WX, Yun LH (1992) *Chin Chem Lett* 3:271
13. Pauling P, Data N (1980) *J Pro Natl Acad Sci USA* 77:708
14. Tripos Inc. (2005) Sybyl 7.1. Manual, St. Louis, MO
15. Chambers JJ, Nichols DE (2002) *J Comput-Aided Mol Des* 16:511
16. McLean TH, Chambers JJ, Parrish JC, Braden MR, Marona-Lewicka D, Kurrasch-Orbaugh D, Nichols DE (2006) *J Med Chem* 49:4269
17. Glennon RA, Young R, Benington F, Morint RD (1982) *J Med Chem* 25:1163
18. Domelsmith LN, Eaton TA, Houk KN, Anderson GM, Glennon RA, Shulgin AT, Castagnoli N, Kollman PA (1981) *J Med Chem* 24:1414
19. Braun U, Braun G, Jacob P III, Nichols DE, Shulgin AT (1978) *NIDA Res Monogr* 22:35
20. Parker MA, Lewicka DM, Lucaites VL, Nelson DL, Nichols DE (1998) *J Med Chem* 41:5148